Tellus (2002), 54B, 713–734
Printed in UK. All rights reserved

TELLUS
ISSN 0280–6509

Three years of aircraft-based trace gas measurements over the Fyodorovskoye southern taiga forest, 300 km north-west of Moscow

By M. RAMONET[1]*, P. CIAIS[1], I. NEPOMNIACHII[2], K. SIDOROV[2], R. E. M. NEUBERT[4], U. LANGENDÖRFER[5], D. PICARD[1], V. KAZAN[1], S. BIRAUD[1], M. GUSTI[1], O. KOLLE[3], E.-D. SCHULZE[3] and J. LLOYD[3], [1]*Laboratoire des Sciences du Climat et de l'Environnement, UMR CEA-CNRS, CE Saclay, Orme des Merisiers, 91191 Gif sur Yvette, France;* [2]*Severtzov Institute of Evolution and Ecology Problems, Russian Academy of Sciences, Lennskii pr. 33, 117071, Moscow, Russia;* [3]*Max Planck Institute for Biogeochemistry, Postfach 100164, 07701, Jena, Germany;* [4]*Centrum voor IsotopenOnderzoek, RUG, Nijenborgh 4, 9747 AG Groningen, The Netherlands;* [5]*Institut für Umweltphysik, Universität Heidelberg (UHEI-IUP), Germany*

(Manuscript received 9 July 2001; in final form 20 June 2002)

ABSTRACT

As part of the EUROSIBERIAN CARBONFLUX project, regular measurements have been performed in the lower troposphere over a southern taiga forest area in Fyodorovskoye, Western Russia (56°28′N, 32°56′E). Up to 70 flights have been made between May 1998 and December 2000, plus additional intensive campaigns to study the diurnal variability of atmospheric trace gases within the boundary layer. We sampled flasks between 100 and 3000 m for analysis of CO_2, $\delta^{13}C$ and $\delta^{18}O$ in CO_2, CH_4 and CO. In addition, in-situ CO_2, relative humidity, pressure and temperature were performed for a better description of the vertical variability and accurate determination of the boundary layer height. The peak-to-peak amplitude of the seasonal cycle of atmospheric CO_2 within the boundary layer of 26.5 ppm is about twice the one observed in the free troposphere (14.6 ppm). The spring draw down of CO_2 also occurs one month earlier than in the free troposphere aloft. There is also an increase by factor of two in the vertical variability of CO_2 within the free troposphere between summer and winter, which may be related to the variability of advection and mixing. Linear regression analysis applied to flask measurements of CO, CH_4 and $\delta^{13}C$ versus CO_2 in the free troposphere indicates that industrial emissions over Europe are a dominant source of synoptic variability in wintertime in air masses reaching Fyodorovskoye. On the other hand, the variability of trace gases in the boundary layer observed during intensive campaigns is consistent with the patterns of proximate sources over the underlying southern taiga landscape at Fyodorovskoye.

1. Introduction

The atmosphere is a well mixed and readily accessible reservoir where CO_2 and long-lived tracer measurements are representative of their sources far away from the sampling site. Although one single atmospheric station makes it possible to characterise the global trend of CO_2 and its variability from one year to the next (Keeling et al., 1989; Enting and Pearman, 1993) a network of stations is necessary to quantify gradients in mixing ratios and to relate them to surface fluxes. An increasing number of flask sampling stations have been installed as part of different air sampling networks in order to downscale carbon fluxes at the scale continents and ocean gyres, using inverse modelling of the atmospheric transport.

Despite a rather abundant literature in inverse modelling, the regional patterns of carbon fluxes is still

*Corresponding author.
e-mail: ramonet@lsce.saclay.cea.fr

uncertain. Although we have very good confidence that the Northern Hemisphere as a whole is a net sink of CO_2 on a decadal mean, large errors remain on the longitudinal apportionment of this sink between ocean and land, and between northern continents themselves. All inversions since Tans et al. 1990 point out to the fact that a substantial fraction of the Northern Hemisphere sink must be located on land, but the contribution of North America vs. Eurasia is still highly uncertain (Bousquet et al., 1999; Fan et al., 1998; Gurney et al., 2002). In a recent study based on 15 atmospheric models that were used to invert annual mean CO_2 gradients, Gurney et al. (2002) inferred a large but moderately uncertain sink over Eurasia (0.4–0.7 GtC yr^{-1}). More interestingly, they also found that the "rectifier" produced by covariance between the seasonal biospheric background flux and atmospheric transport induced a large uncertainty in the inference of boreal Asia fluxes. Boreal Asia is a region where inversions would benefit both from additional observations and from model improvements.

Up to now, very few integrative atmospheric CO_2 measurements have been made on a regular basis over Eurasia (Sugawara et al., 1996; Nakazawa et al., 1997). A primary objective of the EUROSIBERIAN CARBONFLUX project was to establish a climatology of CO_2 and related trace gases over European Russia and Western Siberia. The main purpose of this task was to determine the seasonal cycle of CO_2, and to characterise the annual mean mixing ratio in the interior of the continent with respect to other marine stations already in place in the Northern Hemisphere. In this paper, we present three years of regular aircraft vertical profiles of CO_2 and related tracers at Fyodorovskoye, in European Russia, over a large forested area between Moscow and St Petersburg. Vertical profiles of continuous CO_2 data and flask samples have been obtained in the lower troposphere every three weeks since 1998, and have been completed by three intensive campaigns in summer 1998, summer 1999 and in fall 1999. Vertical soundings at Fyodorovskoye are compared with those of three other aircraft sites in a companion paper (Levin et al., 2002a). We provide here a detailed description of the Fyodorovskoye records, and discuss the implication of measuring CO_2 within and above the boundary layer for validating atmospheric transport models. In addition, the seasonal variation of $\delta^{13}C$ of sources added to the atmosphere is analysed and discussed in light of fossil vs. biospheric contributions. Finally, short-term variability of CO and CH_4 during intensive campaigns is analysed.

2. Sampling site and methods

2.1. Sampling location

Regular vertical profiles were carried out over the Central Forest Reserve (CFR) of Fyoydorovskoye (56°N, 32°E), 300 km north-west of Moscow. The CFR territory is a hilly region (220–280 m a.s.l.) of 245 km^2 (Schulze et al., 2002). It is representative of the Southern taiga biome in Russia, with a mosaic of forests (46% spruce, 26% birch, 14% aspen and 8% pines) and bogs (5%). About 44% of the CFR territory is covered by waterlogged spruce stands with impaired drainage, with drained surfaces amounting to 18%. The remaining surface is made of transition hillsides, flow hollows and closed depressions. Ground-based measurements of net ecosystem exchange (NEE) using the eddy correlation technique (Milyukova et al., 2002) and trace gases mixing ratio within the canopy (Levin et al., 2002b; Langendörfer et al., 2002) were also performed within the CFR territory (Vygodskaya et al., 2002), through different types of ecosystems (150-yr-old spruce forest stand, bog, windthrown spruce forest). The flights were made over the old spruce forest stand (56°28′N, 32°56′E).

2.2. Flight protocol

Flask sampling and CO_2 in-situ measurements were performed on board a bi-plane aircraft Antonov-II, which took off from Moscow or Tver airport. The flights took place at around noon or in the early afternoon, during good weather conditions at a frequency of about every 3 wk (Table 1). Intensive campaigns were also performed during July 1998, July 1999 and October 1999, with two or three flights a day (morning, afternoon, evening), and coincided with ground sampling programmes. Only mid-afternoon (between 12:00 and 17:00 local time) flights are considered in this study for the characterisation of seasonal variations in trace gases. Each profile, going from 100 to 3000 m a.s.l., took about 50 min. Two flask sampling programmes for Laboratoire des Sciences du Climat et de l'Environnement (LSCE) and Centrum voor Isotopen Onderzœk (CIO) were run in parallel.

Three separate air intake lines were installed for an in-situ CO_2 analyser and two flask sampling units of LSCE and CIO. The Antonov-II was also equipped with a system to measure ambient pressure (pressure transducer PTB101B from Vaisala), temperature and humidity (probe HMP35D from Vaisala). The

Table 1. *List of the flights performed at Fyodorovskoye between May 1998 and December 2001*[a]

Day	Month	Year	Time GMT	BL top (m)	Flasks	LICOR Min (ppm)	LICOR Max (ppm)	LICOR Mean (ppm)		LICOR-BL (ppm)		LICOR-FT (ppm)	
18	May	1998	11:43	–	6	–	–	–	–	–	–	–	–
02	Jun	1998	11:01	1650	6	352.7	362.7	357.5	+/− 3.2	354.8	+/− 1.0	360.8	+/− 1.4
24	Jul	1998	06:31	590	9	361.6	393.9	364.7	+/− 6.3	372.2	+/− 12.2	363.0	+/− 0.8
24	Jul	1998	12:37	1900	8	357.2	363.6	361.8	+/− 0.9	361.4	+/− 0.9	362.4	+/− 0.4
28	Jul	1998	06:56	1030	6	349.3	367.7	355.0	+/− 4.2	353.9	+/− 5.7	355.6	+/− 3.1
28	Jul	1998	09:59	1750	6	349.5	359.3	354.7	+/− 3.0	352.4	+/− 1.1	357.8	+/− 1.6
28	Jul	1998	15:18	1390	9	345.1	361.7	353.9	+/− 6.0	347.4	+/− 1.5	359.1	+/− 1.5
29	Jul	1998	06:17	500	8	351.3	364.6	358.9	+/− 3.9	362.2	+/− 3.4	358.3	+/− 3.7
29	Jul	1998	09:50	1300	8	349.5	363.0	355.8	+/− 4.0	352.5	+/− 1.6	359.6	+/− 2.2
29	Jul	1998	14:39	1150	9	348.7	359.8	353.3	+/− 3.4	349.9	+/− 0.8	355.9	+/− 2.1
30	Jul	1998	05:04	800	4	359.7	379.5	366.7	+/− 6.7	377.5	+/− 1.6	362.7	+/− 1.6
30	Jul	1998	15:32	1450	9	348.7	364.6	358.5	+/− 4.0	354.8	+/− 2.6	361.8	+/− 1.3
31	Jul	1998	06:38	350	9	356.1	376.3	360.7	+/− 3.8	367.0	+/− 8.5	360.0	+/− 2.1
31	Jul	1998	09:51	1050	10	354.1	362.0	358.6	+/− 2.6	355.3	+/− 0.6	360.3	+/− 1.4
11	Nov	1998	10:15	470	0	364.2	372.2	367.5	+/− 1.8	370.8	+/− 1.7	366.9	+/− 1.0
24	Nov	1998	10:10	370	0	365.5	419.7	369.6	+/− 6.2	384.2	+/− 11.5	368.0	+/− 1.6
03	Feb	1999	11:09	600	0	–	–	–	–	–	–	–	–
14	Feb	1999	11:12	–	6	–	–	–	–	–	–	–	–
16	Apr	1999	09:20	1250	0	372.0	374.9	373.8	+/− 0.7	374.2	+/− 0.4	373.4	+/− 0.6
28	Apr	1999	09:45	2350	5	369.1	374.5	370.9	+/− 1.4	370.8	+/− 1.4	372.3	+/− 0.3
14	May	1999	11:24	2000	0	372.1	373.9	372.8	+/− 0.4	372.6	+/− 0.2	373.3	+/− 0.2
26	May	1999	06:48	1000	0	362.3	369.1	366.0	+/− 1.8	363.3	+/− 0.8	367.0	+/− 0.7
26	May	1999	15:53	–	0	363.8	366.3	364.4	+/− 0.5	364.4	+/− 0.5	365.1	+/− 0.1
28	May	1999	06:45	1200	0	369.2	371.3	370.3	+/− 0.5	370.7	+/− 0.3	370.0	+/− 0.4
28	May	1999	08:24	1700	0	368.8	370.0	369.5	+/− 0.3	369.3	+/− 0.2	369.6	+/− 0.2
28	May	1999	15:58	2300	0	366.0	371.3	367.6	+/− 1.5	366.7	+/− 0.3	370.0	+/− 0.4
15	Jun	1999	10:23	1600	0	358.8	369.8	364.5	+/− 4.6	360.1	+/− 1.6	369.0	+/− 0.4
28	Jun	1999	10:25	1500	0	356.4	363.4	359.1	+/− 2.2	357.2	+/− 0.4	360.7	+/− 1.7
28	Jul	1999	06:41	2000	10	355.8	363.0	359.5	+/− 2.2	358.1	+/− 1.1	362.1	+/− 0.6
28	Jul	1999	10:26	2270	10	356.3	362.2	358.4	+/− 2.0	357.3	+/− 0.8	361.5	+/− 0.4
28	Jul	1999	16:00	2750	9	–	–	–	–	–	–	–	–
29	Jul	1999	06:05	2220	9	355.2	363.8	359.3	+/− 1.8	358.5	+/− 1.5	361.2	+/− 1.1
29	Jul	1999	10:06	–	10	–	–	–	–	–	–	–	–
29	Jul	1999	15:48	–	10	–	–	–	–	–	–	–	–
30	Jul	1999	10:10	1600	10	352.8	363.9	356.9	+/− 3.5	353.7	+/− 0.5	360.4	+/− 1.1
30	Jul	1999	14:46	2000	10	355.5	365.4	358.4	+/− 2.2	356.9	+/− 1.0	361.1	+/− 0.8

Table 1. *(cont'd)*

Day	Month	Year	Time GMT	BL top (m)	Flasks	LICOR Min (ppm)	LICOR Max (ppm)	LICOR Mean (ppm)		LICOR-BL (ppm)		LICOR-FT (ppm)	
31	Jul	1999	06:23	1650	10	353.7	365.3	359.4 +/−	3.0	357.0 +/−	1.8	362.2 +/−	1.3
31	Jul	1999	10:09	1800	10	355.5	367.0	359.3 +/−	3.4	356.5 +/−	0.6	362.9 +/−	1.6
31	Jul	1999	15:41	2050	10	353.2	362.9	357.3 +/−	3.4	355.0 +/−	1.3	361.7 +/−	1.1
01	Aug	1999	06:04	1150	10	352.1	367.3	357.9 +/−	3.0	354.8 +/−	2.5	359.8 +/−	1.2
01	Aug	1999	09:40	1680	6	352.6	361.8	357.0 +/−	3.3	354.1 +/−	1.4	360.2 +/−	0.6
01	Aug	1999	15:07	1750	9	353.1	362.0	356.6 +/−	3.0	354.2 +/−	0.9	359.8 +/−	1.3
27	Aug	1999	09:09	–	8	–	–	–	–	–	–	–	–
18	Sep	1999	09:22	–	8	–	–	–	–	–	–	–	–
22	Oct	1999	07:42	1500	11	365.2	373.8	366.8 +/−	1.4	367.6 +/−	1.7	366.0 +/−	0.5
22	Oct	1999	11:17	1720	11	365.7	374.3	368.1 +/−	1.5	368.6 +/−	1.7	367.5 +/−	1.0
23	Oct	1999	07:23	1280	13	365.8	373.7	369.3 +/−	1.7	370.4 +/−	1.1	368.5 +/−	1.7
23	Oct	1999	11:19	1030	11	364.1	372.8	367.6 +/−	2.8	371.1 +/−	1.2	366.0 +/−	1.6
24	Oct	1999	08:15	600	6	365.7	373.6	367.6 +/−	1.5	367.3 +/−	0.9	367.7 +/−	1.5
24	Oct	1999	11:21	700	8	366.3	378.4	369.4 +/−	2.9	374.6 +/−	1.7	368.1 +/−	1.2
25	Oct	1999	07:33	980	11	365.1	375.3	369.1 +/−	2.5	372.2 +/−	1.5	367.8 +/−	1.4
25	Oct	1999	10:29	–	5	371.2	375.5	373.7 +/−	1.0	0.0 –	0.0	0.0 –	0.0
25	Dec	1999	09:54	580	6	368.9	376.7	370.8 +/−	1.8	373.5 +/−	2.1	370.3 +/−	1.2
12	Feb	2000	11:12	1350	0	371.7	379.6	374.7 +/−	2.1	376.0 +/−	1.8	373.6 +/−	1.6
29	Mar	2000	10:20	1360	5	369.4	381.2	374.6 +/−	3.6	378.7 +/−	1.4	372.1 +/−	1.8
27	May	2000	10:39	–	5	–	–	–	–	–	–	–	–
05	Jul	2000	09:23	2050	6	349.7	364.5	356.3 +/−	4.4	354.0 +/−	2.6	362.1 +/−	1.5
20	Jul	2000	10:30	–	6	354.6	360.3	358.3 +/−	1.4	358.0 +/−	1.5	359.5 +/−	0.4
03	Aug	2000	08:16	2100	0	356.5	380.2	359.3 +/−	3.9	359.1 +/−	4.7	359.5 +/−	0.4
29	Aug	2000	09:20	1900	0	349.5	365.2	357.2 +/−	5.3	353.3 +/−	2.2	363.5 +/−	1.3
26	Sep	2000	08:09	1450	6	362.7	367.5	365.1 +/−	1.3	366.0 +/−	1.5	364.6 +/−	0.8
07	Oct	2000	10:06	925	6	365.6	384.0	372.6 +/−	6.4	382.3 +/−	1.8	368.8 +/−	2.2
17	Nov	2000	10:40	1950	6	368.4	379.2	374.5 +/−	4.1	377.6 +/−	1.1	369.3 +/−	0.4
01	Dec	2000	11:20	–	5	–	–	–	–	–	–	–	–

[a]For each flight is given: the sampling date, boundary layer height, number of flasks, in-situ CO_2 minimum and maximum mixing ratios between 100 and 3000 m, average CO_2 between 100 and 3000 m, average CO_2 within the boundary layer (BL) and within the free troposphere up to 3000 m (FT). A dash indicates no data, for instance in presence of contamination (see text).

meteorological sensors and the three air inlets were installed along the wire cable used to connect the upper and lower wings. The exhaust of the engine is located on the other side of the cabin, preventing any direct contamination of the measurements. The intake lines were made of about 10 m of Dekabon polyethylene-coated aluminium tubing (6 mm diameter).

2.3. CO_2 in situ measurements

Atmospheric CO_2 dry air mixing ratios were continuously analysed by an NDIR analyser system designed at Max-Planck Institute für Biogeochemie (MPI-BGC) and described in (Lloyd et al., 2002). The NDIR system is based on a LICOR-6251 infrared gas analyser. The air flow through the LICOR was regulated at 1.5 L min^{-1}. The CO_2 mixing ratio was calculated by the customised LICOR software, using the pressure and temperature of the cell. Two calibration gases in high-pressure cylinders were used to regularly recalibrate the data. Calibration gases of 340 and 380 ppm were prepared from ambient air by the Institute fur Umwelt Physik in Heidelberg. Their mixing ratio were related to the primary WMO/CO_2 mole fraction scale maintained at NOAA/CCGG. During the flight, the two calibration cylinders were flown through the LICOR every 500 m during 2 min each, and only the last 10 s were used to calculate the mixing ratios by linearly interpolation. When all flasks are considered, the LICOR minus flask average difference is of -0.11 ± 1.12 ppm. When only flask samples above 2000 m are considered, this difference is of 0.15 ± 1.09 ppm.

2.4. Flask sampling

Duplicate flasks were sampled for LSCE at 2000, 2500 and 3000 m during regular flights. During the intensive campaigns duplicate and single flasks were also sampled at lower levels within the boundary layer between 100 and 2000 m. Duplicate flasks were sampled for CIO at the highest (3000 m) and lowest (100 m) levels. Whole air samples were filled at different altitudes into pyrex glass flasks. Two sampling units were installed for LSCE, Gif sur Yvette (1 L volume flasks equipped with Teflon PFA O-ring valves) and for CIO (2.5 L volume flasks equipped with two viton-O-ring valves). The two sampling units were similar except for the relief valve which was set at 1 bar over ambient pressure for 1 L flasks and 1 bar absolute for 2.5 L flasks. The air was sucked from the inlets at a rate of about 4–5 L min^{-1}. After a flushing time of 5 minutes, the air was compressed in the flasks to the standard target pressure. Pumping is performed by a KNF Neuberger diaphragm pump powered by a 12V DC motor. To dry the air, we use about 10 g of $Mg(ClO_4)_2$ placed in a stainless steel cartridge (diameter 1 cm, length 12 cm), located upstream of the pump and sealed at each end by glass wool plugs. A 1 mm filter is added at the end of the cartridge to avoid entrainment of material inside the sampling unit.

2.5. Flask analysis

The 1 L flasks of LSCE were stored and transported before being analysed, on average 150 d after the sampling. Within the laboratory they were routinely analysed for CO_2 and its isotopic composition ($\delta^{13}C$ and $\delta^{18}O$ ratios), as well as for CH_4 and CO. Stable isotope ratios in CO_2 were measured on a Finnigan MAT252 mass spectrometer. CO_2 was extracted cryogenically from the air contained in the flask using an automatic trapping box system, which included 24 inlet ports and a tunable mass-flow control system (Bourg and Ciais, 1998). An aliquot of about 100 cm^3 of air was necessary to obtain the required amount of CO_2 for mass-spectrometric analysis. Air from each flask sample was firstly flushed through the inlet line for 100 s and then passed into the trapping system with the two cold traps set at $-196\ ^\circ C$. H_2O was separated from CO_2 in two steps by maintaining one trap at $-196\ ^\circ C$ and heating the other at $-80\ ^\circ C$. The desired CO_2 aliquot was then re-condensed in a microvolume trap and injected directly into the mass spectrometer change-over valve via a capillary. The capillary diameter of 0.15 mm ensured constant viscous flow regime, thus preventing systematic fractionation of ^{13}C during the gas inlet into the ionisation chamber. Eight separate acquisitions were made for each sample introduced in the mass-spectrometer against a working standard of pure CO_2. A first amount of 20 L of pure CO_2 working standard was prepared from purified fossil carbonates and industrial CO_2, and its $\delta^{13}C$ ($-9.66‰$) and $\delta^{18}O$ ($-4.77‰$) values were determined against IAEA carbonate reference material and gaseous CO_2 high-pressure cylinders GS-19 and GS-20. Secondary working standards were determined from the primary working standard which is now being used routinely for isotope analysis. The isotope ratio in CO_2 of the working standard currently used is $-8.04‰$ for $\delta^{13}C$ and $-8.14‰$ for $\delta^{18}O$. The isotopic ratios in CO_2 are reported on the V-PDB scale. The isotope ratios were corrected for the effect of N_2O using a fixed value of 310 ppb for N_2O and the measured CO_2 mixing ratio.

Since January 1997 LSCE established an "air scale" by measuring daily two cylinders of dry air using the same extraction protocol as for any routine air sample (air standard 1: $-8.09‰$ for $\delta^{13}C$ and $-5.37‰$ for $\delta^{18}O$; air standard 2: $-8.59‰$ for $\delta^{13}C$ and $-11.50‰$ for $\delta^{18}O$). This provides a quality check for any possible drift of our working standard. The ion correction procedure recommended by Allison et al. (1994) was applied to the data.

The CO_2 mixing ratio within the flasks was measured using an URAS-3G NDIR analyser system (Bourg and Ciais, 1999). The measurement line is made of a manifold of three standard gases and a 24 inlet line for the flasks. A water trap maintained at $-55\ ^\circ C$ was placed in front of the URAS-3G cell. A reference gas flowed continuously through the reference cell (100 mL min^{-1}) of the URAS-3G (47 mL). After manifold had been pumped, the air was allowed to flow through the sample cell of the URAS-3G at a flow rate of 400 mL min^{-1} during 90 s for a 1 L flask sample and during 120 s for a standard gas cylinder. Then the sample cell was isolated and the voltage signal recorded and averaged over 60 s. During a sequence of analysis, each flask was bracketed by three standards against which CO_2 was linearly regressed. The amount of air consumed was about 500 mL, i.e. approximately 25% of each flask content.

The CO mixing ratio was measured at LSCE by gas chromatography on an RGA3 trace analytical gas chromatograph (Gros et al., 1999). Primary standards provided by NOAA/CMDL (CO-in-air, determined against the NOAA/CMDL primary gravimetric scale) were used to calibrate secondary air standards provided by Air-Liquide. Methane analysis was carried out using a GC/FID, and a 2 m long, $1/16''$ diameter packed column (carbosphere 80/100 mesh) at 160 °C. The carrier gas was helium (flow rate 20 cm^3 min^{-1}), and nitrogen was used as a make-up gas at 10 cm^3 min^{-1}(Boissard et al., 1996). The measurements were calibrated with two primary standards from NOAA/CMDL.

The 2.5 L CIO flasks were measured for CO_2, CH_4 and CO by gas chromatography (Hewlett-Packard model 6890, adapted to the special requirements by D. Worthy, AES Environment Canada). CO_2 and CH_4 were separated using a 1.2 m long Haysep Q packed column and detected by a flame ionization detector (FID), CO_2 after being converted into methane in a nickel catalyst with hydrogen. For the separation of CO a different line was employed with a unibead pre-column and a molsieve analytical column, another nickel catalyst methanizer and FID. As the flasks were filled to atmospheric ground-level pressure, the flask air was flushed through the GC inlet sample loops by a small membrane pump. The standard procedure was to measure a reference sample from a tank, two flasks, and another reference sample. The dry air mixing ratios of the reference gas were determined using a suite of three tanks filled and certified by NOAA-CMDL. The calibration of this scale was assessed by the WMO-CO_2 Round Robin experiment as well as by internal EuroSiberian Carbonflux intercomparison experiments.

Due to problems with the flask sampling inlet for LSCE flasks, air samples from October 1998 to June 1999, and during two flights in August 2000, were contaminated. Contamination was easily detected by very high CO and CO_2 mixing ratios. For the LSCE non-contaminated duplicate flasks, the mean pair difference is 0.19 ppm for CO_2, $0.023‰$ for $\delta^{13}C$ in CO_2, $0.069‰$ for $\delta^{18}O$ in CO_2, 4.3 ppb for CH_4 and 3.7 ppb for CO. For the CIO duplicate flasks the mean pair difference is 0.40 ppm for CO_2, 4.0 ppb for CH_4 and 5.3 ppb for CO. The CO_2 mixing ratios measured in the 1 L flasks were corrected for drift during storage. The drift (-0.0012 ppm per day of storage) was estimated from long-term tests performed at CSIRO and MPI-BGC. No consistent drifts were found in the 1 L flasks for CH_4, CO, $\delta^{13}C$ or $\delta^{18}O$ (Levin et al., 2002a), or for the trace gases analysed in 2.5 L flasks. The correction applied to the CO_2 flask data was on average 0.24 ppm (ranging from 0.11 to 0.46 ppm), corresponding to an average storage of 150 d.

3. Typical vertical profiles of CO_2, temperature and humidity

Six vertical profiles are shown in Fig. 1 respectively during and outside the vegetative season. In each case, the top of the atmospheric boundary layer (BL) is detected from the relative humidity and virtual potential temperature profiles, being characterised generally by a sharp decrease of relative humidity, and a slope change in virtual potential temperature. Summertime CO_2 profiles show lower mixing ratios within the BL than aloft, reflecting carbon uptake by photosynthesis. Collocated H_2O profiles (relative humidity) show higher relative humidity values in the BL than aloft, reflecting evapotranspiration. On 15 June 1999 the CO_2 mixing ratio is quite homogeneous in a well mixed BL, with CO_2 mixing ratios being 10 ppm lower than aloft. On 31 July 1999 a well mixed BL again occurs.

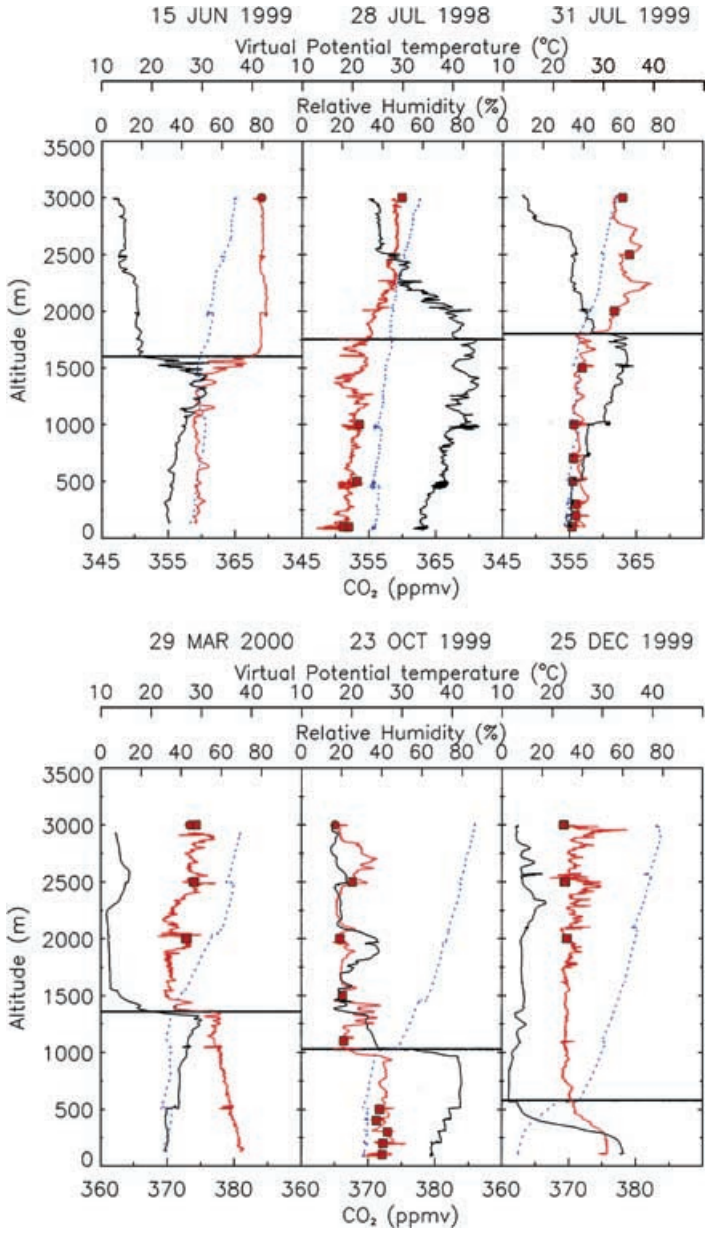

Fig. 1. Typical vertical profiles observed in summer (above) and in autumn, winter and early spring (below) for CO_2 (red line), relative humidity (black solid line) and virtual potential temperature (blue dashed line).

Within the troposphere, peaks of 5 ppm affect the CO_2 profile, which have no counterparts in relative humidity or in temperature. On 28 July 1998 there is a CO_2 increase of about 7 ppm between 100 and 2200 m, with higher variability of CO_2 and relative humidity within the upper part of the BL (1300 and 1700 m).

In winter, the top of the BL lies on average lower than in summer (Fig. 1). Late autumn and winter CO_2 profiles reveal higher CO_2 mixing ratios within the BL than aloft, reflecting CO_2 sources from soil respiration and fossil fuels. On 29 March 2000, CO_2 is observed to decrease between the ground and the top

of the BL, while relative humidity increases. In winter, CO_2 peaks are frequently observed above the top of the BL, associated with atmospheric layers of few 100 m in thickness, as illustrated in the flights of 23 October 1999 and 25 December 1999. Such CO_2 strata, also observed in the air of Siberia (Lloyd et al., 2002) cannot be an artefact of the in-situ LICOR records, since they are confirmed by independent flask points. Such stable layers are reflecting local stratification of the lower atmosphere, and have been frequently observed for pollutants such as CO and CH_4 in aircraft campaigns (Stoller et al., 1999).

4. Seasonal variability

4.1. Back trajectories

In order to illustrate the catchment area of the measurements, we have calculated for each flight the 5-d back trajectories of the air masses sampled at 3000 m, using the Hysplit-4 model (Draxler and Hess 1998). Calculations are based on the 6-hourly archive data from the final run in the series of NCEP operational model runs (FNL archive data). The data are on hemispheric 129×129 polar stereographic grids, and on 14 vertical levels ranging from the surface up to 20 hPa. The vertical motion is calculated from the vertical velocity fields.

Back trajectories calculated for each flight at 3000 m (Fig. 2) indicate that 47% of the air masses sampled come from the north west, 28% from the south west, 1.5% from the south east and 3% associated with air of regional origin (<1000 km from the site). The remaining 20% back trajectories could not be assigned to a single sector. Figure 2 also shows that air sampled at the highest altitude (3000 m) almost exclusively originates from western europe and Scandinavia, whereas air sampled at

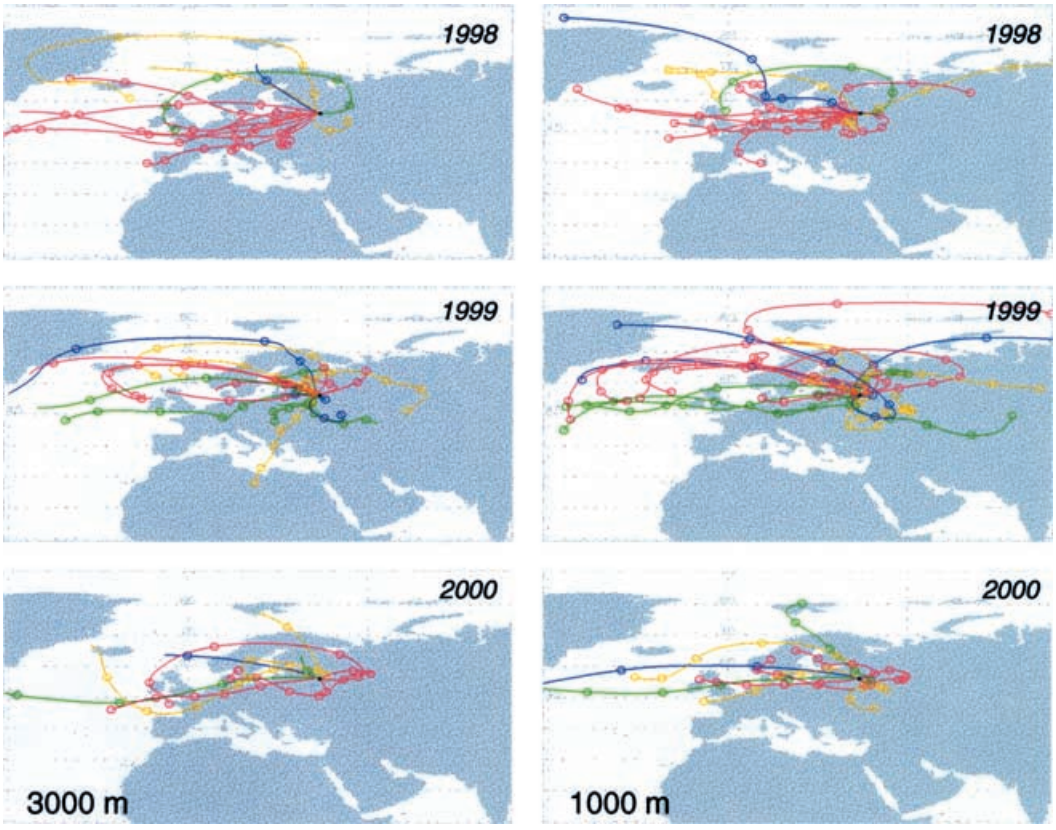

Fig. 2. Five days back trajectories calculated from altitudes 1000 and 3000 m a.s.l. for all flights in 1998, 1999 and 2000. The color indicates the season of the back trajectory: blue for winter, green for spring, red for summer and yellow for autumn.

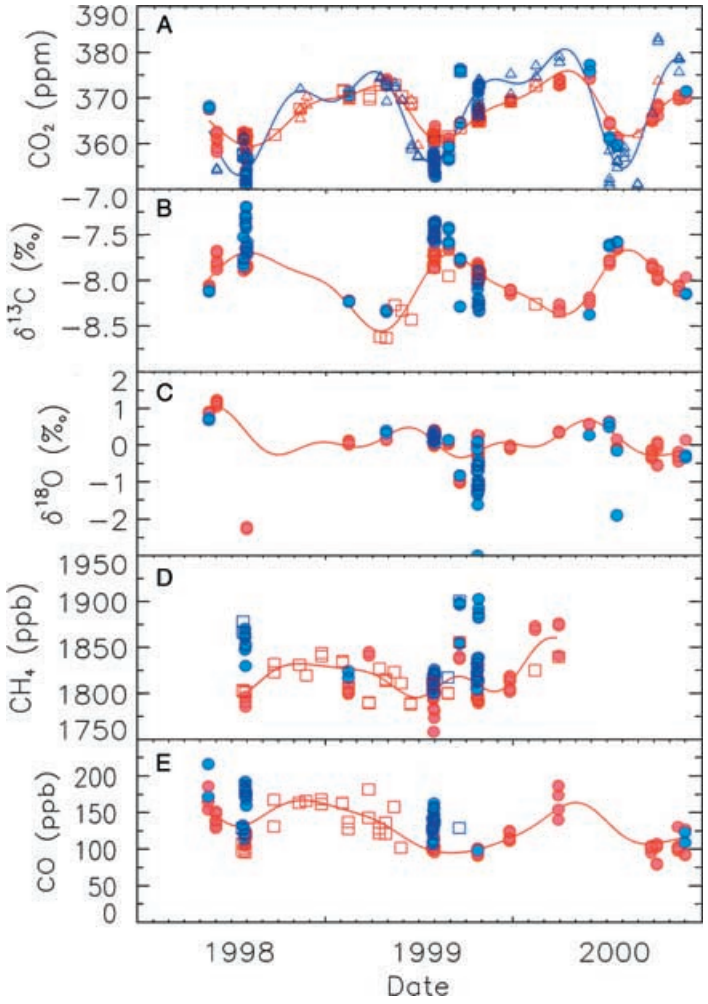

Fig. 3. Time series of (A) CO_2, (B) $\delta^{13}C$ of CO_2, (C) $\delta^{18}O$ of CO_2, (D) CH_4 and (E) CO in the boundary layer (blue) and in the free troposphere (red) at Fyodorovskoye. Circles stand for LSCE flask measurements, squares for CIO flask measurements and triangles for CO_2 in-situ measurements sampled at the intervals of flask sampling.

1000 m also originates from the east, especially in winter.

4.2. *Seasonal variability of CO_2 within and above the boundary layer*

We first sorted out the CO_2 data of each flight into boundary layer (BL) and free troposphere (FT) classes, according to the seasonal variation of the boundary layer top (Fig. 3a). For three flights out of 69 total, it was not possible to determine unambiguously the top of the BL, and in such cases we assigned all CO_2 values above 2500 m to the FT. Also, we excluded from Fig. 3 all morning and evening profiles obtained during intensive campaigns (Table 1). In summer, the BL at Fyodorovskoye is frequently convective, as indicated by the absence of any vertical gradient in virtual potential temperature, and such conditions coincide with well mixed CO_2 mixing ratios within the BL. Interestingly, the top of the mid-afternoon BL in summer lies on average lower at Fyodorovskoye, where it hardly exceeds 2500 m (Fig. 4), than at Zotino in central Siberia, where BL heights of up to 2900 m have been observed (Lloyd et al., 2002). The simulated BL

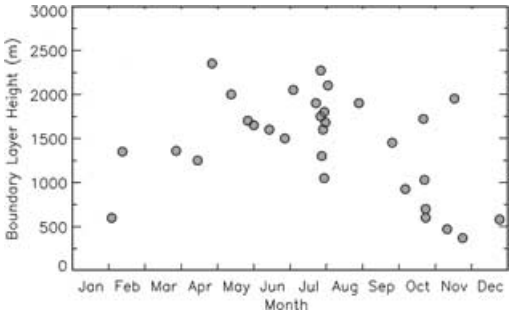

Fig. 4. Boundary layer height estimated from in-situ measurements of pressure, temperature, humidity, and CO_2. Only mid-afternoon (12:00–17:00 LT) flights are considered.

top, as calculated by the regional atmospheric transport model of Kjellström et al. (2002), confirms that the vertical extent of the BL is greater over central Siberia than over European Russia. The most likely explanation is that the growth of BL in central and eastern Siberia is affected by the continuous supply of sensible heat from the forests (Ma et al., 2000). When soils are very dry in summer, Bowen ratios (latent over sensible heat flux) of up to 2–3 have been observed in eastern Siberia (Ohta et al., 2001), and of up to 2.6 over central Siberia, whereas lower Bowen ratios (1.6) prevail in European Russia (Schultze et al., 1999). In addition, frontal systems which advect humidity may inhibit the diurnal growth of the BL, since the vertical turbulence is decreased when overcast sky supresses radiative heating. Such conditions are more frequent in summer in European Russia than in Siberia.

Smoothed time series of CO_2 and trace gases within the BL and the FT, respectively, were constructed by fitting a first-order polynomial term and two annual harmonics to the data. CO_2 is maximum in the FT in mid-April (day 102) and minimum in mid-August (day 223), with an average peak-to-peak amplitude of 14.8 ppm. The BL signal is maximum in early April (day 97) and minimum in late July (day 213), with an average peak-to-peak amplitude of 26.5 ppm. Residuals from the fit, filtered in the time domain with a low-pass filter of full width at half maximum of 150 d, and added back to the fit (Thoning et al., 1989), produced the smoothed curves shown in Fig. 3. A climatology of seasonally varying CO_2 in the boundary layer and in the free troposphere is also given in Fig. 5a. Seasonal variations within the BL reflect the seasonal activity of local sources as selectively observed when flying in mid-afternoon and during fair weather conditions. During the growing season (April to October) the mid-afternoon BL mixing ratio is sensitive to maximum uptake by the vegetation, as shown by collocated flux tower NEE measurements in Fig. 5. At the time of the day when the aircraft flew, the BL convective top also reaches close to its maximum, diluting the sink signal, and creating a positive FT minus BL difference up to 6 ppm in July. Outside the growing season, respired CO_2 accumulates on average within more shallow BL than in summer, yielding to a negative FT minus BL jump down to -5 ppm in November. The seasonal variation of this CO_2 "jump", defined as the difference between FT and BL, can be used to validate the resulting effect of source and sink intensities and vertical mixing in atmospheric transport models (Yi et al., 2002).

We applied an online 3D atmospheric transport model (LMDZ) nudged on ECMWF horizontal wind fields for the year 1998 to compute the CO_2 mixing ratio field due to 3-hourly NEE as simulated globally by the TURC model (Lafont et al., 2002) on a $1^\circ \times 1^\circ$ grid. The NEE fluxes predicted by the TURC model for daytime (noon) and night-time (midnight) are compared with the eddy flux tower measurements in Fig. 5c. The horizontal resolution of the atmospheric transport model is 4° in latitude by 5° in longitude, and the time series of CO_2 mixing ratios were archived over the Fyodorovskoye grid point at all altitudes every 20 min. The atmospheric transport model has 19 vertical levels, including six below 3000 m. The simulated CO_2 mixing ratios were classified into BL or FT values using the virtual potential temperature profile simulated by the online LMDZ model (Hourdin et al., 2002).

Between June and July, the TURC model simulates 40% less uptake than observed (Fig. 5c). The maximum CO_2 uptake (noon NEE) is also simulated to occur one month earlier than observed. This is reflected in the phase of the simulated CO_2 jump in Fig. 5b, which is also in advance by one month, and in the summer amplitude, which is too small compared with the observation. This suggests that TURC underestimates the summer biotic uptake occurs over the whole region which influences the Fyodorovskoye aircraft site, and not just on the grid point where the NEE is measured. Scaling up the TURC simulated NEE everywhere to match the Fyodorovskoye NEE noon observation in July (sensitivity test not shown) would increase the modelled jump, but it still would be underestimated, suggesting that the LMDZ model is mixing up CO_2 too vigorously between the BL and the FT.

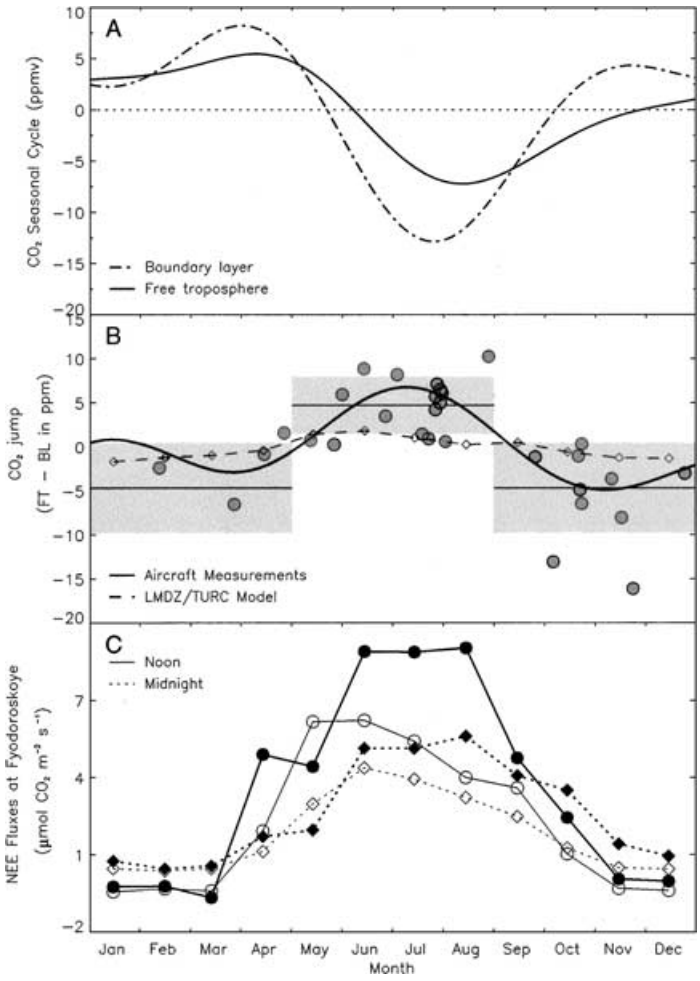

Fig. 5. (A) Average CO_2 seasonal cycle in the boundary layer (dash-dotted line) and in the free troposphere (solid line) obtained from 2.5 yr of vertical profiles. (B) CO_2 "jump" defined as the difference in mixing ratio between the free troposphere and the boundary layer. The circles indicate the "jump" calculated from the in-situ CO_2 measurements reported in Table 1 and the shaded area shows their mean and standard deviation. The solid line indicates the "jump" obtained from the difference between the two smoothed curves in (A). The dash line plus diamonds indicate the modelled "jump" from the three dimensional atmospheric transport model LMDZ selected for mid-afternoon intervals. (C) Eddy covariance Net Ecosystem exchange (NEE) at the Fyodorovskoye 150-yr-old spruce stand forest at noon (solid line and filled circles) and midnight (dotted line and filled circles), compared to the simulated NEE using the TURC light use efficiency model (solid line and open circles). The sign of the noon NEE (negative for uptake) is reversed.

The phase of the BL seasonal cycle of CO_2 is marked by a draw down in May, followed up by an increase in late July, the latter occurring earlier in the BL than in the FT by about 15 d. The standard deviation of the residuals from the smoothed seasonal cycle is higher in the BL (3.65 ppm) than in the FT (1.59 ppm). The CO_2 mixing ratio is indeed more variable in the BL, where the CO_2 residuals from the monthly smoothed curve are governed by hourly changes in boundary layer depth and proximate sources and sinks, than in the FT, where the CO_2 residuals variability reflects synoptic changes in air masses of distinct CO_2 content. The LMDZ model simulated a standard deviation of residuals of 1.53 ppm in the BL, and of 0.77 ppm in the FT when selected for mid-afternoon intervals, thus underestimating the observed variability by

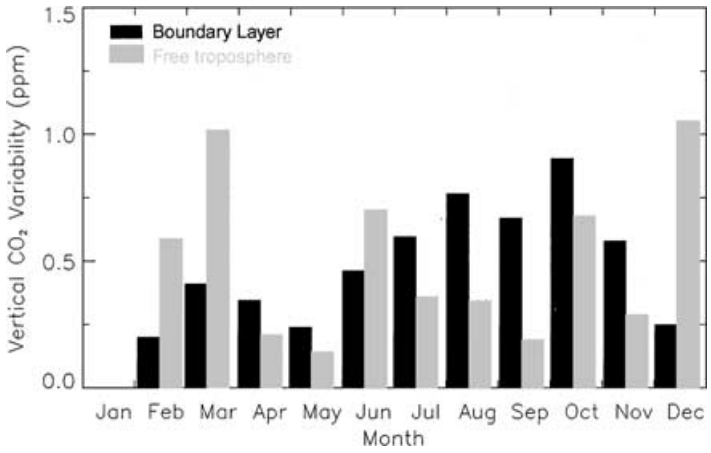

Fig. 6. CO_2 vertical variability within the boundary layer, and in the free troposphere as calculated from in-situ vertical profiles. The vertical variability is calculated as the standard deviation of residuals obtained after substracting for each vertical profile a smooth curve deduced from 50 m averaged data.

approximatively a factor of two, likely because of the coarse horizontal resolution of the model.

4.3. Seasonal variability of CO_2 over small vertical distances

From the LICOR in-situ vertical profiles (acquisition time 1 Hz, corresponding to 1–2 m alongside the CO_2 profile), we calculated the variability of the CO_2 residuals from a smoothed vertical profile obtained by averaging the data in 50 m thick layers. The yearly averaged vertical variance of CO_2, shown in Fig. 6, is identical within the BL (0.5 ± 0.2 ppm) and within the FT (0.5 ± 0.3 ppm). However, the CO_2 vertical variance is greater within the FT than in the BL during the winter, whereas the converse is true during the summer. During winter, the movement of air parcels in stable and residual layers containing pollutants has been observed in the troposphere during various campaigns (e.g. Newell et al., 1999), and more recently such layers were also detected in the case of CO_2 at the three EUROSIBERIAN aircraft sites (this work; Sidorov et al., 2002; Lloyd et al., 2002). Such a seasonal contrast in the variance of CO_2 within the troposphere, which is partly due to the occurence of layers, may be attributed to changes in the intensity and variability of mixing and horizontal advection. The representation of such phenomena in large scale transport models is often poor. From 3-d back trajectories calculated each hour within a month from a point at 3000 m over Fyodorovskoye, we observed a larger scatter in the air parcels origins in winter than in summer, indicating more variable advection. In December, the 3-d origins range over a broader latitude band (35°N–85°N) than in summer (45°N–70°N), and those origins vary more on average from one day to the next than in summer. Broader latitudinal origins of the air parcels in winter than summer cannot be directly translated in terms of more different CO_2 mixing ratio, since the patterns of CO_2 are different. However, the higher space and time variability of the air parcels origins, coupled with the existence of large-scale seasonal gradients in CO_2, might cause greater CO_2 vertical variance in the free troposhere in winter. In summer, however, the CO_2 vertical variance is higher within the boundary layer, where both transport processes and proximal sources activity are more variable.

4.4. Seasonal variability of carbon and oxygen isotopes in CO_2

The time series of $\delta^{13}C$ measured on flask samples mirror the one of CO_2 (Fig. 3b). Unlike for CO_2, where the in situ LICOR records and flasks samples from CIO did complement the LSCE flasks, we only have a limited number of $\delta^{13}C$ flask samples in the BL, which is not sufficient to characterise the $\delta^{13}C$ seasonal cycle. Higher $\delta^{13}C$ values in the BL than in the FT are observed during the vegetative period when CO_2 is conversely lower in the BL, reflecting isotopic enrichment of air in the daytime BL exposed to fractionation by photosynthesis (BL minus FT $= 0.17‰$ between May and August). In winter the situation is reversed, with

higher CO_2 within the BL being mirrored by lower $\delta^{13}C$ values (BL minus FT = −0.11‰), reflecting the input of depleted sources from soil respiration and fossil fuel combustion. The peak-to-peak amplitude of $\delta^{13}C$ in the FT at Fyodorovskoye is of 0.84‰, higher than that obtained at Syktykkar (0.68‰) by Levin et al. (2002a), but in accordance with the higher CO_2 peak-to-peak amplitude at Fyodorovskoye (14.8 ppm vs. 12.4 ppm at Syktyvkar).

$\delta^{18}O$ in atmospheric CO_2 was measured for LSCE flasks but not for CIO flasks. During the intensive campaign in July 1998, insufficient drying of the air led to rejection of most samples with large differences between both members of the same pair (>0.25‰). This problem was corrected in 1999 by doubling the quantity of magnesium perchlorate during the sampling. The available $\delta^{18}O$ data might indicate a seasonal cycle of 1.2‰ in amplitude (Fig. 3c) that is shifted in phase with the CO_2 and $\delta^{13}C$ seasonal cycle. The $\delta^{18}O$ minimum occurs in September–October, whereas the $\delta^{18}O$ maximum occurs between May and June. This phase shift is characteristic of $\delta^{18}O$ at high northern latitudes (Trolier et al., 1996; Ciais et al., 1997; Peylin et al., 1998) and it is explained in global modelling studies by the different phasing of soil respiration, acting in spring and fall to deplete the atmosphere, with respect to photosynthesis, acting in July–August to enrich the atmosphere. The peak to peak amplitude of $\delta^{18}O$ in the FT increases linearly with the peak to peak amplitude of CO_2 between western Europe (Orleans discussed in Levin et al., 2002) and western Russia (Fyodorovskoye, Syktyvkar). On the other hand, in central Siberia (Zotino), the ratio of the $\delta^{18}O$ amplitude to the CO_2 amplitude drops by 30%, suggesting that the isotopic signatures of leaf water and soil moisture in Siberia influence $\delta^{18}O$ in CO_2 to decrease both the mean value and the peak-to-peak amplitude (Cuntz et al., 2002).

4.5. Seasonal variability of CO and CH_4

The CO flask record in the FT shows a seasonal variation, with mixing ratios being on average 60 ppb higher in winter time than in summer time (Fig. 3e). This peak-to-peak amplitude is lower than the one measured at ground-level NOAA/CMDL stations in the Arctic (100 ppb at Alert), and similar to that observed at 3000 m in Orléans (65 ppb). The standard deviation of the CO residuals with respect to the smoothed seasonal curve in Fig. 3 is also very large (22 ppb), indicating contrasted source areas, as well as reflecting the relatively short lifetime of CO, which is not well mixed in the atmosphere. Such scatter is also observed in flask samples at NOAA/CMDL continental ground-level stations in eastern Europe (Baltic Sea = 30 ppb; Black Sea Coast = 65 ppb). In winter, larger CO values likely reflect technological sources over industrialised regions of Europe. In summer, no fossil fuels are used for heating in Russia, but agricultural burning and oxidation of non-methane hydrocarbons may contribute to increased CO (Granier et al., 2000). Photochemical oxidation of CO by OH is, however, greater in summer than in winter. The mixing ratios of CO in the BL measured during intensive campaigns are higher by up to 70 ppb than those in the FT, indicating all year round a strong decrease of CO with height between the surface and the lower troposphere. Such gradients confirm recent model simulations of CO that produce a surface minus 600 hPa difference of 50 ppb in March and 80 ppb in June (Bergamaschi et al., 2000).

The seasonal cycle of CH_4 in the FT shows maximum values in winter and minima in summer, with a peak-to-peak amplitude of 55 ppb, i.e. five times larger than at Syktyvkar over western Siberia (8.1 ppb) and two times larger than at Orléans in western Europe (25 ppb), and comparable to the peak-to-peak amplitude observed at NOAA/CMDL ground stations in western Europe (Baltic Sea = 53.8 ppb) and at high northern latitudes (Alert = 57.5 ppb). In summer, the CH_4 mixing ratios are higher in the BL than in the FT by up to 50 ppb. Such a decrease of CH_4 with height suggests that significant regional CH_4 emissions are acting within the Fyodorovskoye region. In the Central Forest Reserve, natural sources of CH_4 attributable to waterlogged surfaces represent about 44% of the total area. Assuming a summer emission rate of 190 μmol m^{-2} h^{-1} (Neumann, 1999) over 44% of the surface translates into a rate of change of 25 ppb CH_4 per day within a 2000 m thick BL. In addition, anthropogenic emissions from natural gas extraction and distribution, as well as from landfill, may also explain higher values of CH_4 in the BL.

5. $\delta^{13}C$ source signatures

5.1. Variability of $\delta^{13}C$ signature of the sources added to the atmosphere via synoptic transport

We calculated the $\delta^{13}C$ signature (δ_{src}) of the source region influencing each flight via synoptic transport of

air masses (here "source" indicates a flux to or from the atmosphere). To do so, we used the two- component mixing model of Keeling (1961), which makes the assumption that a source of constant signature (δ_{src}) is added through time into an infinite "background" tropospheric air reservoir (C_s) of signature δ_s. The Keeling model has been applied to a wide range of spatial and temporal scales (e.g. Buchmann et al., 1998). In our case, background values C_s and δ_s are taken from the smoothed curve fit to the CO_2 and $\delta^{13}C$ time series at 3000 m (Fig. 3), which defines a continental average contribution (Bakwin et al., 1998). In the approximation where only one source is considered, which implies that fossil fuels and biotic fluxes define δ_{src}, the Keeling model equations stem from the mass conservation of CO_2 and $^{13}CO_2$:

$$C = C_s + C_{src} \tag{1}$$

$$C\delta = C_s\delta_s + C_{src}\delta_{src}. \tag{2}$$

So that

$$C\delta - C_s\delta_s = (C - C_s)\delta_{src} \tag{3}$$

or

$$\delta = -\frac{C_s(\delta_s - \delta_{src})}{C} + \delta_{src}. \tag{4}$$

In the case of an aircraft profile, applying the Keeling model implies that the observed (vertical) gradients in δ and C reflect the addition of δ and C at former points in time along the air mass trajectory. We only retained flask samples above 2000 m in the Keeling model, so as not to account for local sources influencing δ and C at lower levels. For three flights on 14 February 1999, 28 April 1999 and 24 October 1999 it was impossible to determine a significant intercept because the profiles were very stiff, with gradients of less than 0.4 ppm in CO_2 and 0.03‰ in $\delta^{13}C$. For the flight of 1 December 2000 we obtain an intercept of −55‰ which is entirely determined by a large gradient both in CO_2 and $\delta^{13}C$ between the base of the profile and one single flask at 3000 m. An error in the $\delta^{13}C$ of this single sample of 0.04‰, on the order of our experimental precision, would change the intercept value by 6‰. We performed a linear regression analysis on detrended data to determine the intercept in eq. (4) in order to remove influences of the processes related to the long-term variation (e.g. Nakazawa et al., 1993). We applied the Orthogonal Distance Regression analysis (Boggs et al., 1992) to pair-averaged data, accounting for errors in both quantities CO_2 and $\delta^{13}C$ (code "fitexy" in Press et al., 1992). We checked that either the slope of $C\delta$ vs. C or the intercept of δ vs. $1/C$ gives a very similar value for δ_{src}. Results shown in Fig. 7 indicate that δ_{src} varies between

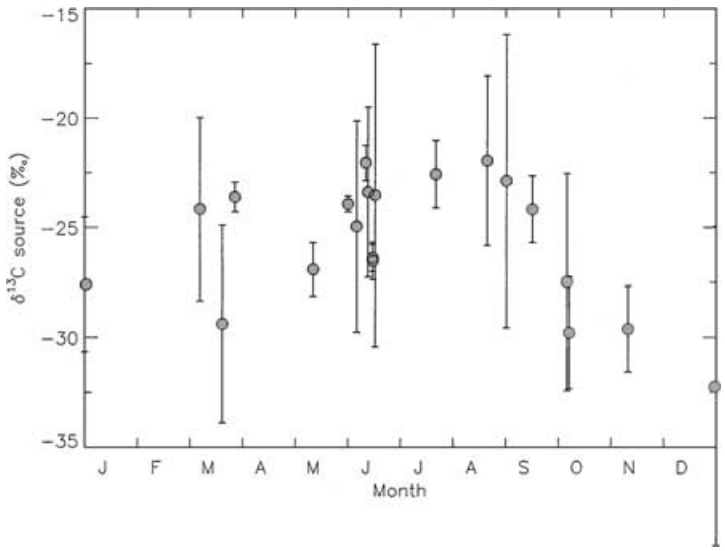

Fig. 7. Apparent $\delta^{13}C$ source signatures calculated from linear regression of $\delta^{13}C$ versus $1/CO_2$ observed in the free troposphere for each aircraft profile. The error bar accounts for errors both in CO_2 and in $\delta^{13}C$. Only flights for which a significant range in $\delta^{13}C$ was observed (>0.05‰), and therefore a significant source signature are shown.

−22‰ and −33‰, with higher values during the vegetative season ($\delta_{src} = -25.0 \pm 2.1$‰ from May to August) and more negative values in autumn and winter ($\delta_{src} = -28.9 \pm 3.3$‰ from October to February). The value of δ_{src} is representative of regional fluxes that have been transported over the last few days before the air mass reaches the site, and it is a weighted value of air depleted in ^{13}C emitted from respiration or fossil fuel burning and of enriched $\delta^{13}C$ due to photosynthetic uptake by plants. The less negative intercept obtained during the growing season is compatible with ecosystem discrimination values. Using an average $d^{13}C$ value above the ABL of 8.0‰ for the growing season yields an average ecosystem discrimination of 16.8‰ for biospheric processes which influence the Fyodorovskoye sampling site above the ABL via long-range transport. Those include the overall effect of canopy photosynthesis and the effect of CO_2 "recycling" both within forest canopies and the overlying ABL (Lloyd et al., 1996). Ecosystem discrimination values reported by Kaplan et al. (2000) are of, respectively, 18 ± 2‰ for cold deciduous species and 20 ± 2‰ for boreal conifer, in the range of our atmospheric based estimate. The samples collected within the ABL at Fyodorovskoye indicate ecosystem discrimination at the landscape level over the Fyodorovskoye forest reserve in a range of 13.0‰ to 27.2‰.

The seasonal variation of δ_{src} at Fyodorovskoye is similar to the one determined at Schauinsland in western Europe by Schmidt et al. (2000) ($\delta_{src} = -24.6$‰ in June–August and $\delta_{src} = -31.2$‰ in January–March) and at Syktyvkar in western Siberia ($\delta_{src} = -25.9$‰ in summer and $\delta_{src} = -30.8$‰ in winter) by Levin et al. 2002, indicating that fossil sources depleted in ^{13}C that are likely related to fossil fuel combustion are present in the winter troposphere over Europe and Siberia in differing amounts with height. Further complication arises from the fact that the fossil fuel mixes used in European countries may have very distinct $\delta^{13}C$ signatures. Figure 2 shows that most of the air masses sampled at Fyodorovskoye in winter originate within 2 d from Russia, Sweden, Poland or northern Germany. In Poland, and to a lesser extent in Germany, coal is the dominant fuel used for electricity production (Marland et al., 2000) and has a typical $\delta^{13}C$ value of −24.1‰ (Andres et al., 1996). On the other hand, in Russia, natural gas burning amounts to almost half of the country's fossil fuel emissions, and has a $\delta^{13}C$ comprised between −46‰ and −50‰ (Galimov et al., 1988). The larger share of natural gas makes the average $\delta^{13}C$ of Russian fossil fuels more negative than anywhere else in western Europe, which is further amplified by the fact that oil-derived fuels in Russia have an average $\delta^{13}C$ of −30‰, as against −26.5‰ for oils imported from the Middle East. In Table 2 we report the average $\delta^{13}C$ of fossil fuels in the source regions influencing the Fyodorovskoye aircraft site, based on energy statistics compiled by Marland et al. (2000) and on the $\delta^{13}C$ signature attached to each type of fuel. It can be observed in Fig. 7 that the winter δ_{src} value of the sources reaching Fyodorovskoye takes an intermediate value between the isotopic composition of fossil fuel in Russia (−34.5‰) and that of nearby countries (range −28.3 to −25.2‰). Interestingly, applying the same analysis as in Fig. 7 to flask data from the Baltic Sea station (located between Poland and southern Sweden) measured by NOAA/CMDL yields a δ_{src} value of −27.2‰ in winter. This less negative intercept reflects the regional influence of coal burning. Overall, when $\delta^{13}C$ is used in 3D atmospheric inversions (e.g. Bousquet et al., 1999; Rayner et al., 1999) to allocate sources and sinks of CO_2 to continents and

Table 2. *National CO_2 emissions from fossil fuel production and cement manufacture in 1996 (Marland et al., 2000) for countries in the source area of Fyodorovskoye*[a]

	Total emissions (10^3 tC yr^{-1})	Gas fuels (%)	Liquid fuels (%)	Solid fuels (%)	Gas flaring (%)	Cement (%)	$\delta^{13}C$ average (‰)
Russian Fed.	43 1090	46.4	21.5	30.7	0.6	0.9	−34.5
Poland	97 375	6.1	13.2	78.7	0.0	1.9	−25.2
Germany	23 5050	19.4	37.4	40.8	0.1	2.3	−28.3
Sweden	14 776	3.1	73.3	21.4	0.0	2.3	−25.9

[a]The average $\delta^{13}C$ of the CO_2 emissions is estimated by using the following estimation for each type of fuel: −44.0‰ for gas fuels, −24.1‰ for solid fuels, −40.0‰ for gas flaring; −30.0‰ for liquid fuels in Russia; −26.5‰ for other liquid fuels; 0.0‰ for cement (Andres et al., 1996).

oceans, a caution flag should be raised on the need to account for regional variations in the composition of fossil fuels, especially in Europe where emissions are high and each country is using a different mix of coal, oil and gas.

Finally, we used repetitive sampling during intensive campaigns (morning, afternoon, evening) to calculate the variation of δ_{src} from one day to the next, based on flask samples taken above the top of the BL. Analysis of the October 1999 campaign showed that the Keeling plot intercept varied little over three consecutive days, and that the day-to-day variability, as well as the variability within a day between morning and evening (1‰) was smaller than the uncertainty on the intercept of each flight. This result is consistent with rather shallow boundary layers at that time, implying little influence of proximate sources on the value of δ_{src}. On the other hand, analysis of the July 1998 and July 1999 campaigns indicate that, even when only flasks taken above the BL top are used in the regression, significant changes in δ_{src} occur within 24 h (up to 3‰), than can be related to the coupling between horizontal advection and the exchange of CO_2 and $\delta^{13}C$ between the BL and the troposphere, via the diurnal growth in BL height or via convective instabilities that have occurred alongside the air mass history.

5.2. *Variability in $\delta^{13}C$ signatures of sources added to the boundary layer at regional and local scales*

We also applied the Keeling model to the intensive campaign data, during which three flights a day were performed (morning, afternoon, evening). Flasks samples from the bottom to the top of the BL were used to determine the isotopic signature of sources added to the BL during daytime. The background values of δ and C were set to those observed during the campaign above the BL, which varied little over the duration of one day, implying no change in air mass. Only profiles with a well defined convective boundary layer (afternoon and evening) were used in the linear ODR regression analysis. The inferred intercept $\langle\delta^{R}_{src}\rangle$ averaged from both afternoon and evening profiles each day reflects the combined isotopic fractionation of respiratory and photosynthetic processes, and within a good approximation it can be used to estimate the regional ecosystem discrimination Δ^{R}_{e}, defined as:

$$\Delta^{R}_{e} = \langle\delta_{B}\rangle - \left\langle\delta^{R}_{src}\right\rangle \quad (5)$$

where $\langle\delta_{B}\rangle$ is the mean $\delta^{13}C$ content in the convective boundary layer (Lloyd et al., 2001). Note that the Keeling model does not allow to identify separately leaf discrimination from the isotopic composition of soil respired CO_2. The regional value of Δ^{R}_{e} derived from BL vertical profiles was compared with the local value independently obtained from canopy measurements (Δ^{C}_{e}). Canopy flask samples were collected each hour at the 150-yr-old spruce stand, 26 m above ground (Langendörfer et al., 2002). We applied the ODR linear regression analysis to canopy flask measurements of CO_2 and $\delta^{13}C$ between sunrise (04:00 UTC) and sunset (15:00 UTC) to calculate the canopy-scale Keeling plot intercept $\langle\delta^{C}_{src}\rangle$, from which the canopy scale ecosystem discrimination (Δ^{C}_{e}) was inferred:

$$\Delta^{C}_{e} = \left\langle\delta^{C}_{B}\right\rangle - \left\langle\delta^{C}_{src}\right\rangle \quad (6)$$

where δ^{C}_{B} is the mean $\delta^{13}C$ value of the lowermost aircraft flask sample (100 m a.s.l.) across the afternoon and evening flights. It can be seen in Fig. 8 that the canopy-scale ecosystem discrimination is on average higher (more positive) than the daytime regional scale ecosystem discrimination by 1.2‰ during the July 1998 campaign and by 2.4‰ during the July 1999 campaign. Night-time canopy flask samples indicate that the $\delta^{13}C$ of soil respired CO_2 at the spruce stand (δ_{r}) equals −27.5‰ in 1998 and −27.95‰ in 1999. Assuming that the night-time value of δ_{r} remains unchanged during the day would yield even higher values of the canopy-scale ecosystem discrimination Δ^{C}_{e} since we would use more negative (by about 1–2‰) values for $\langle\delta^{C}_{src}\rangle$ in eq. (6) (Fig. 8). Comparison between Δ^{C}_{e} and Δ^{R}_{e}, the latter being representative of a larger area over which fluxes are integrated by convective transport in the BL, suggest that ecosystem discrimination at the tower site is relatively more influenced by the addition of CO_2 respired from soils than it is at the regional scale. This observation made at the time of maximum NEE during two campaigns is consistent with the fact that the 150-yr-old spruce stand eddy covariance NEE indicates a net source of CO_2 to the atmosphere even during the vegetative season (Schulze et al., 1999). This source behaviour is related to the site history and to the sensitivity of respiration to temperature (Milyukova et al., 2002), while other ecosystems in the Forest reserve (such as bogs) are observed to be net sinks of atmospheric CO_2. It can also be seen in Fig. 8 that the difference between Δ^{R}_{e} and Δ^{C}_{e} is larger in July 1999 than in July 1998, consistent with respiration maximally exceeding

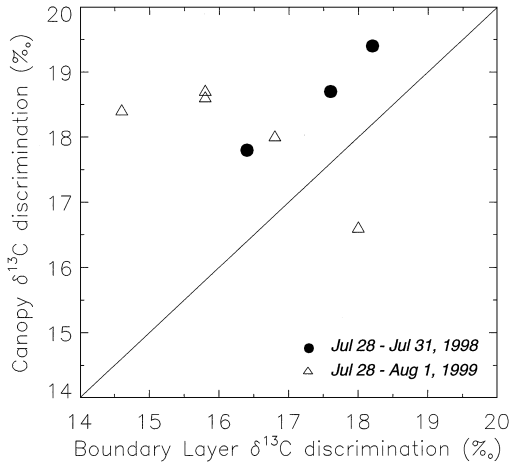

Fig. 8. Ecosystem discrimination calculated in July 1998 (black circles) and July 1999 (open triangles) from linear regression of δ^{13}C versus $1/CO_2$ observed in the daytime convective boundary layer versus the canopy scale ecosystem discrimination calculated from daytime hourly canopy flask samples taken 26 m above ground at the 150-yr-old spruce stand where eddy covariance NEE is measured.

photosynthesis in 1999, one of the hottest summers on record, whereas 1998 was cooler than the long-term average (Milyukova et al., 2002).

6. Correlations between CO_2 and CO or CH_4

6.1. Variability of CO and CH_4 in the free troposphere as compared with CO_2

Analysis of CH_4 and CO made it possible to study the relationship between those species and CO_2 in the troposphere. In winter, CO and CH_4 have mainly industrial sources which should parallel fossil CO_2 emissions. In summer, however, CO is additionally destroyed by OH radicals and produced by the oxidation of hydrocarbons, whereas additional biogenic CH_4 sources are attributable to the decomposition of domestic waste, wetlands emissions and agricultural activities. We analysed the ODR linear regression lines between CH_4 and CO_2 and between CO and CO_2 in Fig. 9. Residuals from the detrended smoothed curves in Fig. 3 were regressed against each other for each pair of species to obtain $\Delta CH_4/\Delta CO_2$ and $\Delta CO/\Delta CO_2$ ratios. As expected, there is no correlation in summer between CO, CH_4 and CO_2 residuals (Fig. 9) because those three species have distinct source and sink patterns. Nevertheless, Nakazawa et al. (1997) found a negative correlation between CH_4 and CO_2 from vertical profiles between 500 and 6000 m across Siberia in summer, which they attributed to the coincidence of an increase of CO_2 with height (plant uptake) and a decrease of CH_4 with height (biogenic emissions). Our data do not show such pattern because they do not resolve the vertical structure of trace gases, but rather are related to synoptic changes in air masses delivering air from distinct source regions. In winter (October–April), the $\Delta CH_4/\Delta CO_2$ ratio of 9.5 ± 2.4 ppb CH_4 per ppm CO_2 is very similar to the one observed at the two other aircraft sites in Western Siberia (10 ppb CH_4 per ppm CO_2 at Syktyvkar) and in

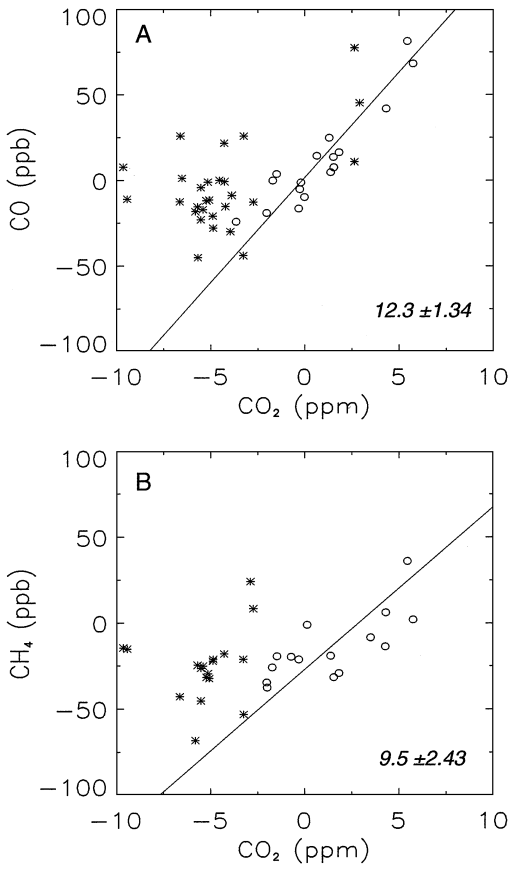

Fig. 9. (A) Relationship observed in summer (crosses) and winter (open circles) within the free troposphere between the CO and CO_2 residuals from the smoothed seasonal fits shown in Fig. 3. (B) Same for the relationship between CH_4 and CO_2.

central Siberia (9.77 ppb CH_4 per ppm CO_2 from the four "polluted flights" discussed in Lloyd et al., 2002). The $\Delta CO/\Delta CO_2$ ratio of 12.3 ± 1.3 ppb CO per ppm CO_2 at Fyodorovskoye is higher than the values determined for "polluted flights" over central Siberia by Lloyd et al. (8.81 ppb CO per ppm CO_2) and by Harris et al. (2000) at Barrow, Alaska for polluted air masses in winter (7.9 ppb CO per ppm CO_2). On the one hand, higher soil respiration rates expected during winter in European Russia than in central Siberia would act to lower the value of the $\Delta CO/\Delta CO_2$ ratio at Fyodorobskoye, but this site also lies closer to industrial sources of CO in western Europe and Russia, which is reflected in the higher observed $\Delta CO/\Delta CO_2$ ratios. Indeed, industrial emissions compiled by EMEP/CORINAIR (http://www.emep.int/emissions.htl) and averaged over Western European countries plus the Ukraine and Russia indicate that a CO to CO_2 ratio in industrial sources of 12.28 ppb CO per ppm CO_2 in 1998 (13.4 over Western Europe only), a value that is very close to the $\Delta CO/\Delta CO_2$ ratio observed in the lower troposphere at Fyodorovskoye. This suggests that the variations in observed CO_2 mixing ratios are largely a consequence of variations in the amount of fossil CO_2 attributable to industrial sources.

6.2. *Variability of CH_4 and CO in the boundary layer in July 1998 and 1999*

During intensive campaigns, boundary-layer CO and CH_4 mixing ratios have been measured in flask samples, with typically six flask samples in the BL part of the aircraft profile. There is a marked difference in the BL content of various trace gases between the two summer campaigns carried out during July 1998 and July 1999, respectively. In July 1998, the CO mixing ratios within the BL and in the FT above were similar. In fact, the forest reserve area was not strongly influenced by fossil sources during the campaign, despite the relative proximity of Moscow (300 km to the south east) because air masses originated from the west. In the mean time, an accumulation of CH_4 in the BL was measured, with a BL minus FT difference of 25 ± 14 ppb CH_4, the large scatter mostly reflecting a change in air mass by 28 July associated with the passage of a low-pressure system. Inspection of 5-d back trajectories indicated otherwise westerly winds. July 1998 was cooler and remarkably wetter than the long-term average, with twice as much precipitation. Consequently, very shallow water tables were observed (Levin, personal communication) that promoted anaerobic decomposition and CH_4 emissions from soils. Indeed, CH_4 fluxes measured in static chambers were up to four times higher in July 1998 (100–1500 μmol m^{-2} h^{-1}) than in July 1999 (0–300 μmol m^{-2} h^{-1}) in a bog site near the forest eddy flux tower (Neumann, 1999). In July 1999, on the other hand, we observed a large CO accumulation in the BL in the morning, with CO mixing ratios being higher by 50 ppb than in the air aloft. Such a build-up of CO became diluted in the daily growth of the BL, but was still discernible in the afternoon and evening profiles. Hot and relatively dry conditions in July 1999, one of the hottest summers on record, coincided with forest fires: one such fire was observed visually from the airplane within the forest reserve area, and several others further to the West. During the campaign, air masses originated from the north west (Scandinavia) until 30 July and then from the north east (Arctic).

Figure 10 shows CO vs. CO_2 and CH_4 vs. CO within the BL in July 1998 and 1999 (morning, afternoon and evening profiles). The picture is consistent with high rates of CH_4 emissions from wet soils and bogs in July 1998, and with CO and CH_4 emissions from fires in July 1999. The $\Delta CO_2/\Delta CO$ and $\Delta CH_4/\Delta CO$ ratios were calculated, using the morning boundary layer as an integrator of surface fluxes (Table 3). The average $\Delta CH_4/\Delta CO$ ratios of 0.11 ± 0.03 ppb CH_4 per ppb CO during the fire episode of July 1999 (excluding the flight of 28 July with no significant correlation between both species) lies within the range of emission factors previously determined in the smoke of various boreal forest fires: 0.05–0.07 ppb CH_4 per ppb CO after Cofer et al. (1998) and 0.03–0.17 ppb CH_4 per ppb CO after Andreae and Merlet (2001). The $\Delta CO_2/\Delta CO$ ratios observed during the fire episode (23 ± 10 ppb CO per ppm CO_2) are however, much higher than those determined in boreal fire plumes (range 7–13 ppb CO per ppm CO_2), being additionally influenced by respired CO_2 which accumulated from the previous night in the morning BL.

7. Conclusions

We carried out regular aircraft soundings of the lower troposphere over a southern taiga forest in Fyodorovskoye, western Russia, as a concerted action within the EUROSIBERIAN CARBONFLUX project. This results constitute one of the very few regular aircraft datasets available over Eurasia. Vertical

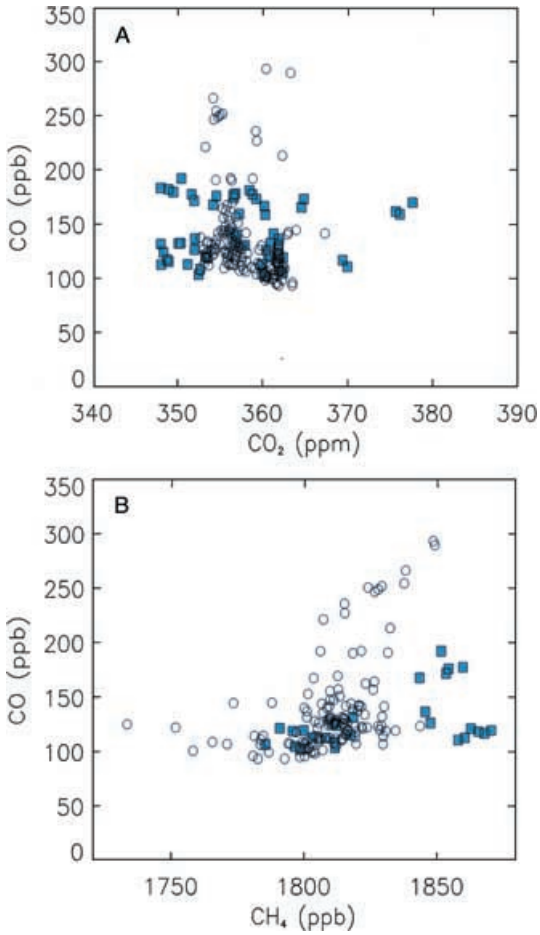

Fig. 10. (A) CO versus CO_2 mixing ratio, and (B) CO versus CH_4 mixing ratios within the boundary layer during the two intensive campaigns in July 1998 (squares) and July 1999 (open circles).

profiles were sampled between 100 and 3000 m every 3 wk between May 1998 and December 2000. Both in-situ CO_2 measurements and flask samples were obtained. Despite rejection of many contaminated flasks, and a long turnover (150 d) of flasks, requiring important storage corrections, when carefully putting together two independent flask records and the in-situ CO_2 data it was possible to describe the seasonal variation of CO_2, $\delta^{13}C$ and $\delta^{18}O$ of CO_2, CH_4 and CO in the free troposphere. In the case of CO_2, the atmospheric boundary layer was sampled as well as the free troposphere aloft. The top of the boundary layer varied between 500 m in winter and up to 2500 m in summer. Collocated time series of the CO_2 difference between the free atmosphere and the boundary layer, and of the eddy covariance NEE, provide a useful constraint on the covariance between vertical mixing in the lower atmosphere and biospheric fluxes, a process known as the "seasonal rectifier". In linkage with the seasonal variability of atmospheric transport, we also observed that in winter there is much more vertical structure in the CO_2 profiles in the free troposphere. Only in-situ CO_2 measurements could reveal such variability, which may reflect the occurrence of stable layers, together with more variable horizontal advection fields in winter. In such a case, pointwise flask sampling may yield to incorrect representation of the mean CO_2 content of the atmosphere between two levels, as being simulated by atmospheric transport models. Finally, we analysed the synoptic variability of CO, CH_4 and $\delta^{13}C$ in air masses that are added to the mean seasonal cycle. The CO to CO_2 and CH_4 to CO_2 regression lines were only significant in winter, and reflected the input of industrial emissions. Similarly, $\delta^{13}C$ of the apparent sources added to the atmosphere was significantly lower in winter than in summer, which can be explained by the addition of isotopically depleted fuels burned in Russia, especially natural gas.

Three years of regular aircraft soundings at Fyodorovskoye represent a new piece of information for better retrieving regional carbon sources and sinks in models. However, considering the large variability in distribution of trace gases in the continental atmosphere, an increase of the network will be needed over Boreal Asia for reliable estimation of regional carbon fluxes. Along those lines, it would be most helpful to acquire regular measurements within the boundary layer as well as in the free atmosphere, in order to characterize the seasonal variability of trace gases near the surface. Boundary layer data will be valuable in global inversions, although they would require atmospheric models of increased resolution, which account for diurnal cycles of NEE as well as for boundary layer transport processes. Since the realism, and the spatial and temporal resolution, of transport models will likely improve in the future, it is important to start such measurements whenever possible.

8. Acknowledgements

We thank all those who helped with the Fyodorovskoye airborne sampling program. In particular we thank the crew of the Antonov-II for all the flights performed during these 3 years. We thank N.N.

Table 3. *Differences in CO, CH_4 and CO_2 mixing ratiosfrom the top ofthe boundary layer during the morning flights (July 1998 and July 1999)*[a]

Date	Time LT	ΔCO (ppb)	ΔCH_4 (ppb)	ΔCO_2 (ppm)	AltMax (m)	*N*	$\Delta CO_2/\Delta CO$ (mol/mol)	*r*	$\Delta CH_4/\Delta CO$ (mol/mol)	*r*
28 Jul 1998	10	13.3	56.3	17.5	500	4	1429.7	0.6	4.66	0.7
29 Jul 1998	9	−4.2	−1.8	13.1	500	2	–	–	–	–
30 Jul 1998	9	9.5	–	1.7	500	2	183.5	1.0	–	–
28 Jul 1999	10	30.6	20.1	10.6	700	5	287.7	0.8	0.37	0.5
29 Jul 1999	10	91.2	8.6	5.9	300	2	64.8	1.0	0.09	1.0
31 Jul 1999	10	98.7	14.2	2.9	500	4	28.7	0.9	0.15	0.9
1 Aug 1999	10	186.4	19.3	10.5	500	4	52.0	0.9	0.11	0.9

[a]A positive difference an accumulation in the boundary layer. Linear regression lines between CO_2 and CO and between CH_4 and CO are calculated for each flight, number of flask samples (*N*), slopes and correlation coefficient (*r*).

Vygodskaya and her colleagues for their advice and support; Martin Heimann for the coordination of the EUROSIBERIAN CARBONFLUX project; Uwe Langendorfer for conditioning of the Eurosibs' flasks; and C. Valant, M. Grall, G. Monvoisin and R. Sarda-Esteve for the flask analysis. We are also grateful to P. Tans (CMDL/NOAA) and J. White and B. Vaughn (INSTARR) for giving access to the results of the Baltic Sea sampling site. This project has been partly funded by the European Commission under ENV4-CT-97-0491 and by the Max-Planck-Gesellschaft, München, Germany.

REFERENCES

Allison, C. E., Francey, R. J. and Meijer, H. A. 1994. Recommendations for the reporting of stable isotope measurements of carbon and oxygen in CO_2 gas. in *Proceedings of IAEA consultants' meeting, 1–3 December 1993*, IAEA, Vienna.

Andreae, M. O. and Merlet, P. 2001. Emission of trace gases and aerosols from biomass burning. *Global Biogeochem. Cycles* **15**, 955–966.

Andres, R. J., Marland, G., Boden, T. and Bishoff, S. 1996. Carbon dioxide emissions from fossil fuel combustion and cement manufacture 1751–1991 and an estimate of their isotopic composition and latitudinal distribution. In: *Global change institute* (ed. T. Wigley and D. Schimel). Cambridge Univ. Press, Aspen, Co.

Bakwin, P., Tans, P. P., White, J. W. C. and Andres, R. J. 1998. Determination of the isotopic ($^{13}C/^{12}C$) discrimination by terrestrial biology from a global network of observations *Global Biogeochem. Cycles* **12**, 555–562.

Bergamaschi, P., Hein, R., Heimann, M. and Crutzen, P. J. 2000. Inverse modeling of the global CO cycle 1. Inversion of CO mixing ratios. *J. Geophys. Res.* **105**(D2), 1909–1927.

Boggs, P. T., Byrd, R. H., Rogers, J. and Schnabel, R. 1992. ODRPACK Version 2.01, Software for Weighted Orthogonal Distance Regression. (Applied and Computational Mathematics Division.)

Boissard, C., Bonsang, B., Kanakidou, M. and Lambert, G. 1996. TROPOZ II: Global distributions and budgets of methane and light hydrocarbons. *J. Atmos Chem.* **25**, 115–148.

Bourg, C. and Ciais, P. 1998. Mesure haute précision par spectrométrie de masse des rapports isotopiques $\delta^{13}C$ et $\delta^{18}O$ du dioxide de carbone, DSM-LSCE, CEA Saclay. Report no. CEA-R-5796.

Bourg, C. and Ciais, P. 1999. Mesure automatisée de la concentration en CO_2 d'air atmosphérique prélevé dans des flacons, DSM-LSCE, CEA Saclay. Report no. CEA-R-5873.

Bousquet, P., Ciais, P., Peylin, P., Ramonet, M. and Monfray, P. 1999. Inverse modelling of annual atmospheric CO_2 sources and sinks, 1, Method and control inversion. *J. Geophys. Res.* **104**(D21), 26 161–26 178.

Buchmann, N. and Ehleringer, J. R. 1998. CO_2 concentration profiles, and carbon and oxygen isotopes in C-3, and C-4 crop canopies. *Agric. Fore. Meteorol.* **89**, 45–58.

Ciais, P., Dening, A. S., Tans, P. P., Berry, J. A., Randall, D. A. and coauthors, 1997. A three dimensional synthesis study of $\delta^{18}O$ in atmospheric CO_2. 1. Surface fluxes. *J. Geophys. Res.* **102**(D5), 5857–5871.

Cofer III, W. R., Winstead, E. L., Stocks, B. J., Goldhammer, J. G. and Cahoon, D. R. 1998. Crown fire emissions of CO_2, CO, H_2, CH_4, and TNMHC from a dense jack pine boreal forest fire. *Geophys. Rese. Lett.* **25**, 3919–3922.

Conway, T. J., Tans, P. P., Waterman, L. S., Thoning, K. W., Kitzis, D. R., Masarie, K. A. and Zhang, N. 1994. Evidence for interannual variability of the carbon cycle from the National Oceanic and Atmospheric Administration/Climate Monitoring and Diagnostic Laboratory Global Air Sampling Network. *J. Geophys. Res.* **99**(D11), 22 831–22 855.

Cuntz, M., Ciais, P. and Hoffman, G. 2002. Modelling the continental effect of oxygen isotopes over Eurasia. *Tellus* **54B**, this issue.

Draxler, R. R., and Hess, G. D. 1998. Description of the Hysplit-4 modeling system. *NOAA Technical Memorandum ERL ARL-224*.

Enting, I. G., and Pearman, G. I. 1993. Average global distributions of CO_2. In: *The global carbon cycle* (ed. M. Heimann). NATO ASI Series, 31–64.

Fan, S.-M., Gloor, M., Mahlman, J., Pacala, S., Sarmiento, J., Takahashi, T. and Tans, P. 1998. A large terrestrial carbon sink in North America implied by atmospheric and oceanic carbon dioxide data and models. *Science* **282**, 442–446.

Galimov, E. M. 1988. Sources and mechanisms of formation of gaseous hydrocarbons in sedimentary rocks. *Chem. Geol.* **71**, 77–95.

Granier, C., Petron, G., Muller, J. F. and Brasseur, G. 2000. The impact of natural and anthropogenic hydrocarbons on the tropospheric budget of carbon monoxide. *Atmos. Environ.* **34**, 5255–5270.

Gros V., Bonsang, B. and Sarda Esteve, R. 1999. Atmospheric carbon monoxide 'in situ' monitoring by automatic gas chromatography. *Chemosphere* **1**, 153–161.

Gurney, K. R., Law, R. M., Denning, A. S., Rayner, P. J., Baker, D. and coauthors, 2002. Towards robust regional estimates of CO_2 sources and sinks: using atmospheric tranport models. *Nature* **415**, 626–630.

Harris, J. M., Dlugokencky, E. J., Oltmans, S. J., Tans, P. P., Conway, T. J., Novelli, P. C., Thoning, K. W. and Kahl, J. D. W. 2000. An interpretation of trace gas correlations during Barrow, Alaska, winter dark periods, 1986–1997. *J. Geophys. Res.* **105**(D13), 17 267–17 278.

Hourdin F., Couvreux F. and Menut, L. 2002. Parametrisation of the dry convective boundary layer based on a mass flux representation of thermals. *J. Geophys. Res.* in press.

Kaplan, J. O., 2001. Geophysical applications of vegetation modeling. *PhD Thesis*, Lund University, Sweden, Department of Ecology, p. 128.

Keeling, C. D. 1961. The concentrations and isotopic abundances of atmospheric carbon dioxide in rural and marine air. *Geochem Cosmochim. Acta* **24**, 277–298.

Keeling, C. D., Bacastow, R. B., Carter, A. F., Piper, S. C., Whorf, T. P., Heimann, M., Mook, W. G. and Roeloffzen, H. A. 1989. A three-dimensional model of atmospheric CO_2 transport based on observed winds, 1. Analysis of observational data. In: *Aspects of climate variability in the Pacific and Western Americas, Geophysical Monogr. Ser.* (ed. D. H. Peterson). AGU, Washington, DC, **55**, 165–236.

Kjellström, E., Holmén, K., Eneroth, K. and Engardt, M. 2002. Summertime Siberian CO_2 simulations with the regional transport model MATCH: A feasibility study of carbon uptake calculations from EUROSIB data. *Tellus* **54B**, this issue.

Lafont, S., Kergoat, L., Dedieu, G., Chevillard, A., Karstens, U. and Kolle, O. 2002. Spatial and temporal variability of land CO_2 fluxes estimated with remote sensing and analysis data over western Eurasia. *Tellus* **54B**, this issue.

Langendörfer, U., Cuntz, M., Ciais, P., Peylin, P., Bariac, T., Milukova, I., Kolle, O. and Levin, I. 2002. Modeling of biospheric CO_2 gross fluxes via oxygen isotopes in a spruce forest canopy: an ^{222}Rn calibrated box model approach. *Tellus* **54B**, this issue.

Law, R., Rayner, P. J., Denning, A. S., Erickson, D., Heimann, M., Piper, S. C., Ramonet, M., Taguchi, S., Taylor, J. A., Trudinger, C. M. and Watterson, I. G. 1996. Variations in modeled atmospheric transport of carbon dioxide and the consequences for CO_2 inversions. *Global Biogeochem. Cycl.* **10**, 783–796.

Levin, I., Ciais, P., Langenfelds, R., Schmidt, M., Ramonet, M., Sidorov, K., Tschebakova, N., Gloor, M., Heimann, M., Schulze, E. D., Vygodskaya, N. N., Shibistova, O. and Lloyd, J. 2002a. Three years of trace gas observations over the EURO-Siberian domain derived from aircraft sampling—a concerted action. *Tellus* **54B**, this issue.

Levin, I., Born, M., Cuntz, M., Langendörfer, U., Mantsch, S., Naegler, T., Schmidt, M., Varlagin, A., Verclas, S. and Wagenbach, D. 2002b. Observations of atmospheric variability and soil exhalation rate of radon-222 at a Russian forest site: Technical approach and deployment for boundary layer studies. *Tellus* **54B**, this issue.

Lloyd, J., Kruijt, B., Hollinger, D. Y., Grace, J., Francey, R. J. and coauthors, 1996. Vegetation effects on the isotopic composition of atmospheric CO_2 at local and regional scales: Theoretical aspects and a comparison between rain forest in Amazonia and a boreal forest in Siberia. *Aust. J. Plant Physiol.* **23**, 371–399.

Lloyd, J., Francey, R. J., Mollicone, D., Raupach, M. R., Sogachev, A. and coauthors, 2001. Vertical profiles, boundary layer budgets, and regional flux estimates for CO_2 and its $^{13}C/^{12}C$ ratio and for water vapor above a forest/bog mosaic in central Siberia. *Global Biogeochem. Cycl.* **15**, 267–284.

Lloyd, J., Langenfelds, R., Francey, R. J., Gloor, M., Tschebakova, N. N., Zolotukhine, D., Werner, R. A., Jordan, A., Allison, C. A., Zrazhewske, V., Shibistova, O. and Schulze, E. D. 2002. A trace gas climatology above Zotino, central Siberia. *Tellus* **54B**, this issue.

Ma, X. Y., Fukushima, Y., Hiyama, T., Hashimoto, T. and Ohata, T. 2000. A macro-scale hydrological analysis of the Lena River basin. *Hydrol. Proc.* **14**, 639–651.

Marland, G., Boden, T. A. and Andres, R. J. 2000. Global, regional, and national fossil fuel CO_2 emissions. In: *Trends: A compendium of data on global change*. Carbon Dioxide Information Analysis Center, Oak Ridge National Laboratory, US Department of Energy, Oak Ridge, Tenn.

Milyukova, I., Kolle, O., Varlagin, A., Vygodskaya, N., Schulze, E-D. and Lloyd, J. 2002. Carbon balance of a southern taiga spruce stand in European Russia. *Tellus* **54B**, this issue.

Nakazawa, T., Morimoto, S., Aoki, S. and Tanaka, M. 1993. Time and space variations of the carbon isotopic ratio of tropospheric carbon dioxide over Japan. *Tellus* **45B**, 258–274.

Nakazawa, T., Sugawara, S., Inoue, G., Machida, T., Makshyutov, S. and Mukai, H. 1997. Aircraft measurements of the concentrations of CO_2, CH_4, N_2O and CO and the

carbon and oxygen isotopic ratios of CO_2 in the troposphere over Russia. *J. Geophys. Res.* **102**(D3), 3843–3859.

Neumann, E. 1999. Methanemissionen aus natürlichen Feuchtgebieten, *Staatsexamensarbeit, Institut für Umweltphysik,* Universität Heidelberg.

Newell, R. E., Thouret, V., Cho, J. Y., Stoller, P., Marenco, A. and Smit, H. G. 1999. Ubiquity of quasi-horizontal layers in the troposphere. *Nature* **398**, 316–319.

Ohta, T., Hiyama, T., Tanaka, H., Kuwada, T., Maximov, T. C., Ohata, T. and Fukushima, Y. 2001. Seasonal variation in the energy and water exchanges above and below a larch forest in eastern Siberia. *Hydrol. Proc.* **15**, 1459–1476.

Peylin, P., Ciais, P., Denning, S., Tans, P. P., Berry, J. A. and White, W. C. 1998. A three-dimensional study of $\delta^{18}O$ in atmospheric CO_2: contribution of different land ecosystems. *Tellus* **51B**, 642–667.

Press, W. H., Teukolsky, S. A., Vetterling, W. T. and Flannery, B. P. 1992. Numerical recipes in Fortran 77. In: *The art of scientific computing,* 2nd edn. Cambridge University Press.

Rayner, P. J., Enting, I. J., Francey, R. J. and Langenfelds, R. 1999. Reconstructing the recent carbon cycle from atmospheric CO_2, delta C-13 and O_2/N_2observations. *Tellus* **51**, 213–232.

Schmidt, M., Neubert, R., et al. 2001. Variability of CO_2 and its stable isotope ratios at Shauinsland (Germany) and Neumayer (Antarctica). Sixth International CO_2 Conference, Sendai, Japan.

Schulze, E. D., Lloyd, J., Kelliher, F. M., Wirth, C., Rebmann, C. and coauthors, 1999. Productivity of forests in the Eurosiberian boreal region and their potential to act as a carbon sink—a synthesis. *Global Change Biol.* **5**, 703–722.

Schulze, E.-D., Vygodskaya, N. N., Tschebakova, N., Czimczik, C. I., Kozlov, D., Lloyd, J., Mollicone, D., Parfenova, E., Sidorov, K., Varlagin, A. and Wirth, Ch. 2002. The Eurosiberian Transect: An introduction to the experimental region. *Tellus* **54B**, this issue.

Sidorov, K., Sogachev, A., Langendörfer, U., Lloyd, J., Nepomnjashiy, I. L., Vygodskaya, N., Schmidt, M. and Levin, I. 2002. Seasonal variability of greenhouse gases in the lower troposphere above the eastern European Taïga (Syktyvkar, Russia). *Tellus* **54B**, this issue.

Stoller, P., Cho, J. Y. N., Newell, R. E., Thouret, V., Zhu, Y. and coauthors, 1999. Measurements of atmospheric layers from the NASA DC-8 and P-3B aircraft during PEM-Tropics A. *J. Geophys. Res.* **104**(D5), 5745–5764.

Sugawara, S., Nakazawa, T. and Khattatov, V. U. 1996. Aircraft measurements of the stable carbon isotopic ratio of atmospheric methane over Siberia. *Global Biogeochem. Cycl.* **10**, 223.

Tans, P. P., Fung, I. Y., et al. 1990. Obeservational constraints on the global atmospheric CO_2 budget. *Science* **247**, 1431–1438.

Thoning, K. W., Tans, P. P. and Komhyr, W. D. 1989. Atmospheric carbon dioxide at Mauna Loa Observatory, 2. Analysis of the NOAA GMCC data, 1974, 1985. *J. Geophys. Res.* **94**(D6), 8549–8565.

Trolier, M., White, J. W. C., Tans, P. P., Masarie, K. A. and Gemery, P. A. 1996. Monitoring the isotopic composition of atmospheric CO_2: Measurements from the NOAA global air sampling network. *J. Geophys. Res.* **101**(D20), 25 897–25 916.

Vygodskaya, N. N., Schulze, E.-D., Tchebakova, N. M., Karpachevskii, L. L., Kozlov, D., Sidorov, K. N., Panfyorov, M. I., Abrazko, M. I., Shaposchnikov, E. S., Solozeva, O. N., Minaeva, T. Y., Jeltuchin, A. S., Wirth, C. and Pugachevshii, M. Y. 2002. Climatic control of stand thinning in unmanaged spruce forests of the southern taiga in European Russia. *Tellus* **54B**, this issue.

Yi, C., Davis, K., Bakwin, P., Denning, A. S. and Zhang, N. 2002. Is the simulated forcing of the CO_2 rectifier effect too strong? *J. Geophys. Res.* in press.